Steel and Composite Structures, *Vol. 14, No. 5 (2013) 493-509*
DOI: http://dx.doi.org/10.12989/scs.2013.14.5.493

Ultimate behavior of composite beams with shallow I-sections

Selçuk Emre Görkem*[1] and Metin Hüsem[2]

[1]*Erciyes University, Biosystems Engineering Department, Kayseri, Turkey*
[2]*Karadeniz Technical University, Civil Engineering Department, Trabzon, Turkey*

(Received February 04, 2013, Revised April 22, 2013, Accepted May 20, 2013)

Abstract. Bending behavior of reinforced concrete slabs encased over shallow I-sections at different levels of compression heads were investigated in present study. 1500 mm long I-sections were used to create composite slabs. Compression heads of monolithic experimental members were encased at different levels into the concrete slabs. Shear connections were welded over some of the I-sections. The testing was carried out in accordance with the principles of four-point loading. Results revealed decreasing load bearing and deflection capacities of composite beams with increasing encasement depths into concrete. Mechanical properties of concrete and reinforcing steel were also examined. Resultant stresses calculated for composite beams at failure were found to be less than the yield strength of steel beams. Test results were discussed with regard to shear and slip effect.

Keywords: composite beam; shear connectors; ultimate behavior; collapse mechanism

1. Introduction

Steel is usually preferred as an effective construction material because of lightness, performance and speed of construction. However, it has some disadvantages like poor fire and corrosion resistance and expensiveness. In steel structures, steel and concrete are used together in order to decrease construction cost and to increase strength and to achieve high fire resistance. Therefore, composite members are commonly used in constructions to has created today's composite structural technique (Knowles 1973, Davies 1975).

Steel is commonly used in combined with other materials. For instance, bridge decks have been built prefabricated or monolithic reinforced concrete slabs. In order to increase fire resistance, steel columns and beams are encased in to the concrete. In multi-storey buildings and bridges, composite beams are commonly used in order to benefit from compressive strength of concrete and tensile strength of steel (Salmon and Johnson 1971, Chen *et a*l. 2007). Composite beams are built with the help of shear connectors on steel beams or with embedding steel beams in to the concrete partly or totally (Cai *et al*. 2007, Ranzi *et al*. 2006).

Composite construction is used extensively in modern building and highway bridges. A composite construction may provide about 30-50% savings in weight of steel and a significant increase in load-bearing capacity and relative stiffness. Such a composite members may also yield significant decreases in total height of a building (Ranzi and Zona 2007).

*Corresponding author, Assistant Professor (Ph.D.), E-mail: gorkem@erciyes.edu.tr

Copyright © 2013 Techno-Press, Ltd.
http://www.techno-press.org/?journal=scs&subpage=8 ISSN: 1229-9367 (Print), 1598-6233 (Online)

1.1 Composite Interaction

Increase in load-bearing capacity is involved in interaction between steel beam and slab. Beam reaches maximum load-bearing capacity in case of full interaction. Additionally, stress distribution throughout the cross-section becomes uniform. Steel beam and reinforced concrete slab carry loads together in a composite case and advantages of composite construction emerge. If there is no interaction, steel beam bears all the service loads plus the weight of concrete slab (Knowles 1973, Davies 1975, Salmon and Johnson 1971).

Between two extreme cases, full interaction and non-composite beams, there is a case named, incomplete interaction or partial interaction. In this case, stress distribution is not uniform over the cross-section. There are two neutral axes both in slab and steel beam. A part of concrete slab is exposed to tension. Mostly a little slippage occurs at interface between steel beam and concrete slab, but it is much smaller compared to non-composite beams. Slip has significant effect on internal behavior of beams (Chen *et al*. 2007, Cai *et al*. 2007). In some cases, interaction may be classified as longitudinal and transverse interaction (Ranzi *et al*. 2006) and shear deformability of steel components may be effective on overall composite beam performance (Ranzi and Zona 2007).

The theoretical and experimental studies on composite beams have been published since 1920s. Kahn J. secured a patent called composite beam structure in 1926. Since then, the behaviors of composite beams, composite curved beams and shear connectors have been investigated by several researchers (Arda and Yardimci 2000, Galambos 2000, Byfield *et al*. 2004, Liang *et al*. 2004, Fabbrocino *et al*. 2000, Nie and Cai 2003, Thevendran *et al*. 2000, Viest *et al*. 1958, Johansen 1970, Johansen 1972, Heins 1976, Hamada and Longworth 1976, Ansourian 1981, Fahmy 1996, Gattesco 1999, Fabbrocino *et al*. 2001, Dall'asta 2001, Lee and Kim 2010, Chung and Lawson 2001, Shanmugam *et al*. 2002, Amadio and Fragiacomo 2002, Nakamura and Narita 2003). However, few studies have been published on the behavior of composite beams with regard to encasement ratio of steel into concrete.

In this study, bending behavior of reinforced concrete slabs encased over shallow I-sections at different levels of compression heads were investigated Reinforced concrete slabs were encased over compression flanges of 1500 mm long shallow I-sections at various levels. Some of the experimental members were designed with shear connections. Incomplete interaction cases were investigated through with thick-slab composite beams, shallow steel beams and different shear connector combinations. The testing was carried out in accordance with the principles of four-point loading.

2. Experimental study

2.1 Steel beams

In this study, 1500 mm long, 100 mm high I-section steel beams were used in composite beams. Bending tests were conducted on beams and Young modulus and yield strength values were determined as E_s = 302, 63 MPa, F_y = 369, 88 MPa, respectively.

2.2 Geometrical properties of composite beams and shear connectors

2.2.1 R/C slab

Table 1 Mechanical properties of reinforcement steel

Diameter (mm)	Yield strength (N/mm^2)	Tension strength (N/mm^2)	Rupture strain (%)
8	520	630	18

Fig. 1 Reinforcing steel mesh on a composite beam with stud shear connector

2.2.2 Reinforcement

Wire mesh reinforcement with 8 mm bars was used within reinforced concrete slab. Bars were installed at 100 × 165 mm spacing. Mechanical properties were examined and given in Table 1. Reinforcements, embedded in slab symmetrically, 20 mm from top and bottom, are presented in Fig. 1.

2.2.3 Encased sections

Cross-sections and characteristics of encased sections denoted by “*E*” are provided in Table 2. Size of *R*/*C* slab is h = 125 mm, b = 250 mm and L = 1500 mm.

*E*4 has same geometrical properties as *E*3, but it has additional shear connectors. In *E*4 series, it was aimed to observe the effect of shear connectors in encased sections**.** In production of experimental specimens, compressive flange of the steel beam was embedded 50 mm (*E*1 series), 30 mm (*E*2 series), 10 mm (*E*3 series), and 10 mm with shear connectors (*E*4 series) into the concrete slab. In *E*4 series, the bolts with 10 mm diameter and 105 mm height were used as shear connectors. Shear connectors are presented in Fig. 2.

Table 2 Cross-sections and properties of encased sections

Beams	Cross-sections	Section properties
Steel beam (*E*0)	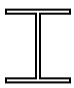	100 mm high steel beam

Table 2 Continued

1st Series beams (*E*1)	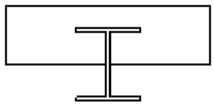	50 mm encased
2nd Series beams (*E*2)	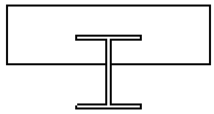	30 mm encased
3rd Series beams (*E*3)	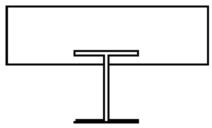	10 mm encased
4th Series beams (*E*4)	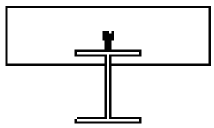	10 mm encased with shear connectors

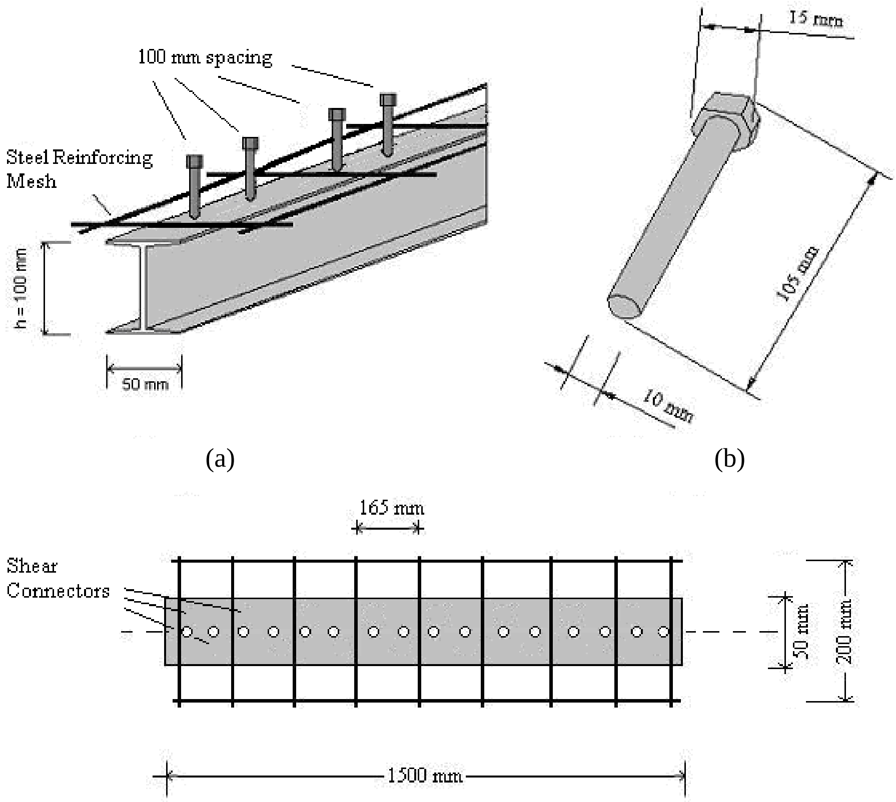

(c)

Fig. 2 Steel beam, reinforcing bars and shear connectors

2.2.4 Non-encased sections

Four different types of connectors were used in non-encased sections denoted by “*K*”. Sizes and images of channel, angle, stud and box connectors are presented in Figs. 3 and 4, respectively.

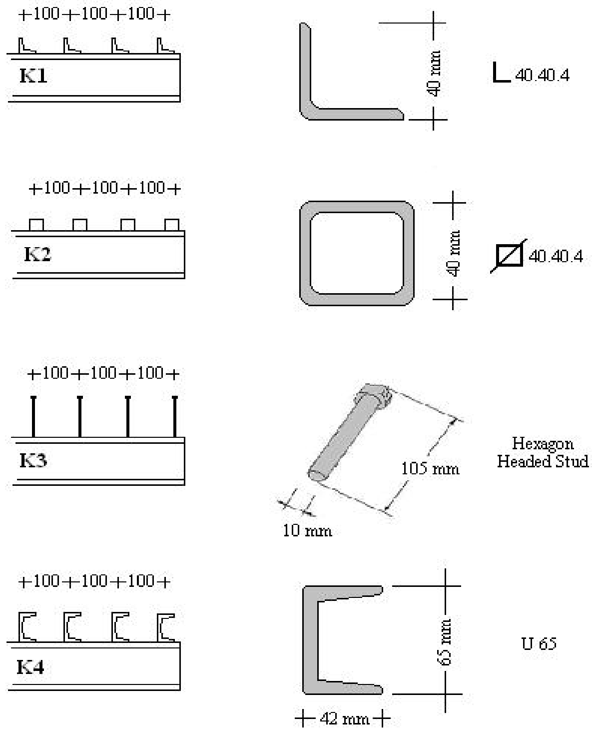

Fig. 3 Composite beams and shear connectors

Fig. 4 Non encased test specimens

2.2.5 Materials properties and mix design for concrete

Limestone aggregate with 16 mm maximum diameter were proportioned and used in concrete mixture (TS 706 1985). Physical properties of aggregate (TS 3526 1985) can be seen in Table 3. CEM IIIA 32.5 cement and super-plasticizer (about 1% of cement volume) were used in miture.

Mixing proportions of concrete (TS 802 1985) are given in Table 4.

Compressive strength characteristics of corresponding beams (determined over 3 cylinder specimens with d = 150, h = 300 mm) are given in Table 5. The differences between compressive strength values were not more than 5%. Two strain gauges were used to determine Young Modulus (E_c) and Poisson's ratio (v) of concrete. Strain gauge (120 mm) were placed orthogonal directions to determine longitudinal and circumferential strains. Fig. 5 shows stress-strain relationship for concrete. Poisson's ratio were found to be $v = 0{,}242$. Compressive strength, E_c (TS 500 2000) and modular ratios are provided in Table 5.

Table 3 Physical properties of aggregate

Aggregate size	Loose density (kg/m^3)	Dry density (kg/m^3)	Saturated density (kg/m^3)	Water absorption (%)
Course (> 4 mm)	1445	2706	2720	0,43
Fine (< 4 mm)	1485	2675	2682	0,50

Table 4 Mixing proportions of concrete

W/C	Cement (kg/m^3)	Water (kg/m^3)	Total aggregate (kg/m^3)	Absorbed water (kg/m^3)	Admixture
					SP (kg/m^3)
0.50	350	175	1828.5	4.2	35

Table 5 Strength values for concrete and steel

Specimen	Compressive strength (MPa)	Young modulus ($MPa*10^3$)	Modular ratio $n = E_s / E_c$
$E1$	36	33,77	8,962
$E2$	38	34,03	8,892
$E3$	38,5	34,93	8,824
$E4$	38	34,03	8,962
$K1$	38,5	33,90	8,927
$K2$	37,5	33,77	8,962
$K3$	37	34,16	8,859
$K4$	38	34,03	8,893

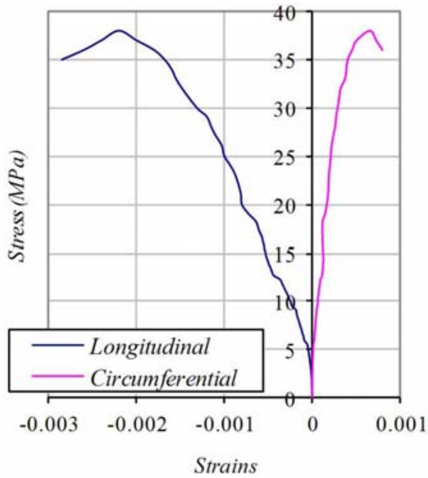

Fig. 5 Stress-strain relationship of concrete

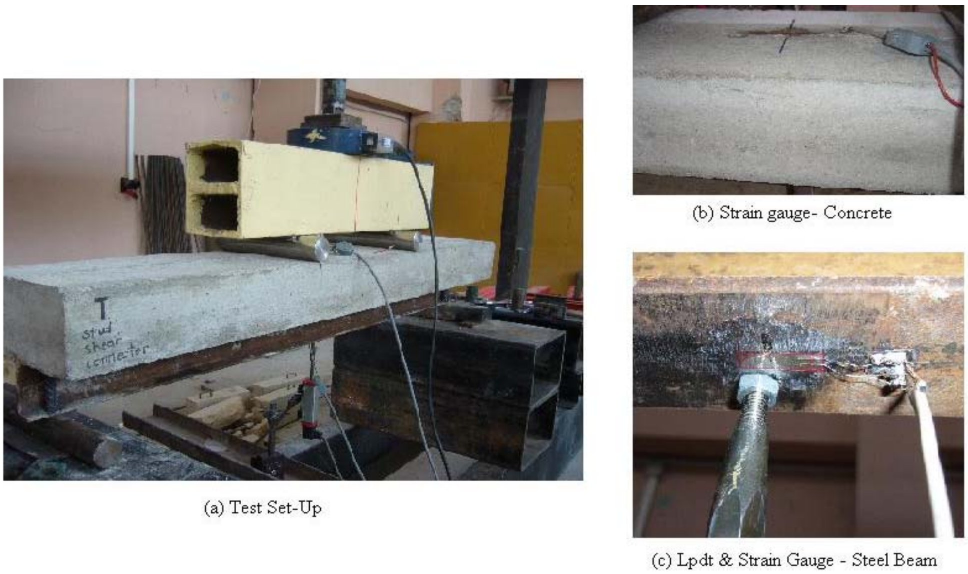

Fig. 6 Test set-up and measurement devices

2.3 Test set-up and measurement devices

Beams were tested in their 28th day. Tests were performed under four-point loading and set-up can be seen in Fig. 5. Loads recorded by using 500 kN capacity load cell. Strains and midspan deflections at corresponding loading level were measured by using 20 mm capacity strain gauges and 100 mm capacity linear potentiometric displacement transducers. Strain gauges were placed at concrete surface and steel beam at midspan. In composite beam tests, strain gauge with 90 mm measurement length was placed on the top of concrete slab (compression region) and another strain gauge with 20 mm measurement length was placed on the bottom (tensile region) of I-section steel beams. The experiment set up for bending tests are presented in Fig. 6.

3. Test results and calculations

Deflections, failure loads, maximum strains and failure moments at ultimate loading level are given in Table 6.

As seen in Table 6, the lowest load was recorded in specimen with angle shear-connectors. Composite beam with box connectors had 12%, stud had 18.5%, and channel had 20.3% higher ultimate loads than the beam with angle connectors.

Table 6 Test results at ultimate loading

Specimen	Deflections (mm)	Failure loads (kN)	Maximum strains		Failure moments (kN.m)
			Concrete (Top)	Steel (Bottom)	
*E*0 (steel beam)	15,0	46	-0,0024	0,0024	12,65
*E*1	7,0	75	-0,0012	0,0018	18,75
*E*2	8,1	100	-0,0019	0,0040	25,00
*E*3	10,6	110	-0,0014	0,0042	27,50
*E*4	13,4	129	-0,0023	0,0046	32,25
*K*1 (angle)	5,373	133,83	-0,00092	0,001593	33,50
*K*2 (box)	7,021	152,99	-0,00112	0,002022	38,25
*K*3 (stud)	11,11	164,12	-0,00157	0,0030	41,03
*K*4 (channel)	10,04	167,83	-0,00151	0,002341	41,95

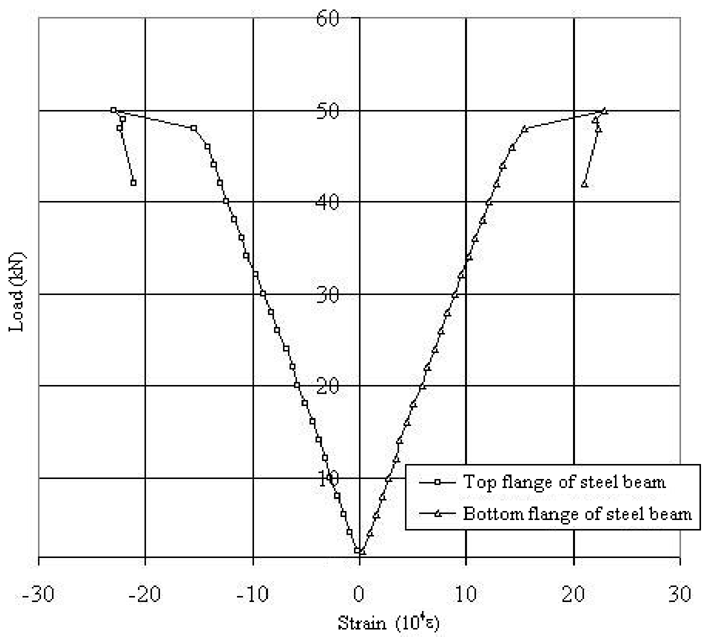

Fig. 7 Steel beam’s load-strain graphic

Load-bearing capacity of the 3rd series beams (concrete slab encased 10 mm - without shear connector) was 47% more than *E*1 series composite beams (concrete slab encased 50 mm) and that of the *E*2 series beams was 33% more than *E*1 series composite beams.

Load bearing capacity of *E*4 series composite beams with shear connectors (concrete slab embedded 10 mm) was 15% more than the *E*3 series composite beams produced without shear connectors (concrete slab embedded 10 mm). Such results revealed an average 15% increase in load-bearing capacity with shear connectors.

The average ultimate deflection of composite beams decreased with increasing embedment of concrete slabs (see Table 8). For instance, the average deflection in *E*3 series composite beams (concrete slab encased 10 mm) was 51% more than *E*1 series composite beams (concrete slab embedded 50 mm).

Steel beam's load-strain graphic is presented in Fig. 7.

Load and strain values were measured in each test specimens. The average load-strain relationships for all encased test beams are provided in Fig. 8.

*E*1 series beams steel yielding was observed before the fracture of composite beam since shear connection between steel and concrete was not achieved in these series without shear connectors. In the other series of composite beams, the effect of concrete compressive strength was increased with decreasing embedment depth. It was seen that the decrease of embedding depth increased the deflection and load bearing capacity of beams.

Load-deflection relationships for *K* series beams are presented in Fig. 9 and load-strain relationship are given in Fig. 10.

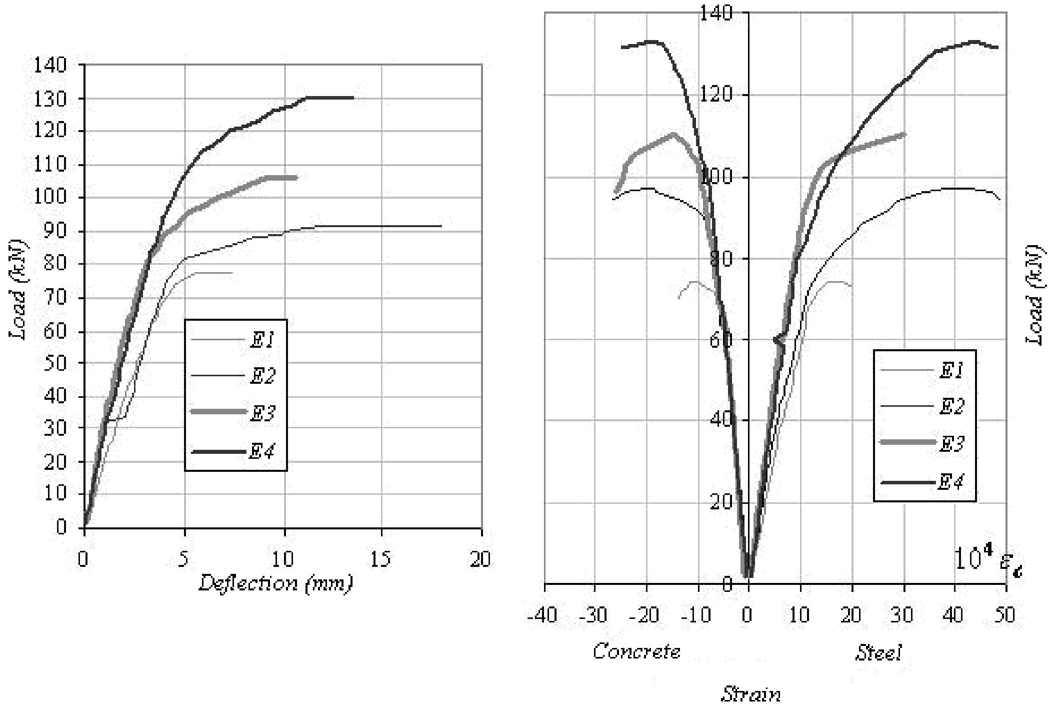

Fig. 8 Load-deflection and load-unit deformation curves of composite beams

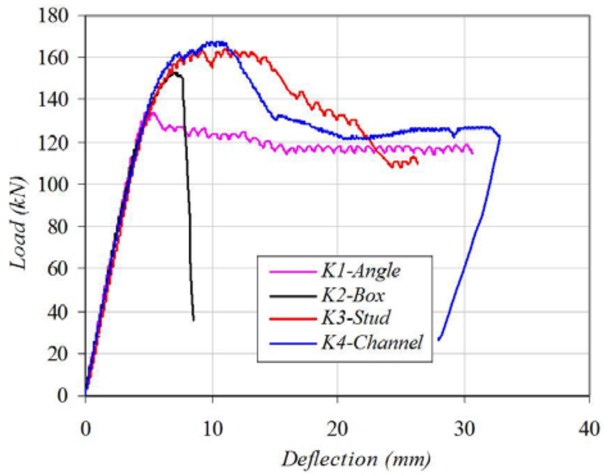

Fig. 9 Load-deflection relationship of composite beams

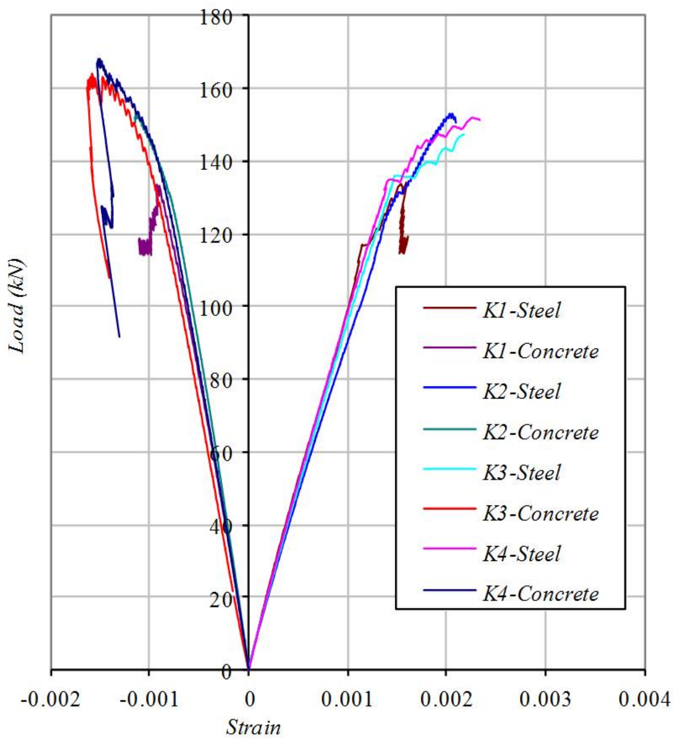

Fig. 10 Load-strain relationships of composite beams

3.1 Shear interaction in encased sections

Location of neutral axis, moment of inertia and section modulus were determined to evaluate shear interaction in encased sections and corresponding values are given in Table 7.

Table 7 Cross-sectional properties and stress calculations

Specimen	Neutral axis from top (cm)	Moment of inertia (cm^4)	Section modulus (cm^3)
*E*0 (steel beam)	-	171	34,2
*E*1	7,707	928,77	94,84
*E*2	8,160	1182,89	104,31
*E*3	8,610	1489,25	115,54
*E*4	8,180	2101,07	157,74
*K*1 (angle)	8,610	1709,51	129,4
*K*2 (box)	8,180	1680,04	125,0
*K*3 (stud)	9,060	1780,23	127,6
*K*4 (channel)	9,290	1744,7	129,4

In encased cross-sections, load is carried at a plane along a-b-c-d region (Fig. 11(a)). Bonding force and transverse shear were effective along b-c (compression flange) and longitudinal shear was effective along a-b and c-d lines.

If a cross section is able to bear shear force, bond strength at b-c region must be limited to 0.03 f_c, bond strength along a-b and c-d regions is limited to 0.12 f_c. Additionally, if there is no reinforcement bars placed under compressive flange in encased cross sections, it is assumed that these regions are not able to bear load (Mergulhao *et al*. 1998). Such a region can be seen in Fig. 11(b). *Q*-static moment was calculated by using the neutral axis of cross sections and the area shown in Fig. 7(b) was not included into calculations. *t* is equal to total shear-transmitting length of a-b,b-c and c-d. $v = VQ / It$ represents shear stress at ultimate loading conditions.

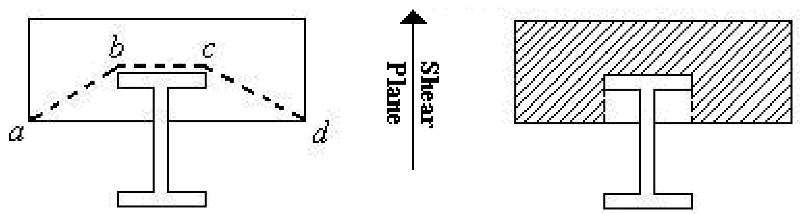

(a) (b)

Fig. 11 Shear force transmission in encased sections

Table 8 Shear calculations

Series	Shear forces P/2 (kN)	b-c (cm)	a-b = c-d (cm)	Shear stress at failure $v = V.Q / I.t$ (N/mm^2)	Total shear strength along a-b, b-c and c-d 0,15 f_c (N/mm^2)
*E*1	37,5	5	11,18	65,67	5,4
*E*2	50	5	10,44	101,80	5,7
*E*3	55	5	10,05	120,15	5,8
*E*4	64,5	5	10,05	99,87	5,7

Fig. 12 Shear cracks in test specimens

Excessive shear stresses were observed in specimens (Table 8). Therefore, circumstance failure of cross sections were occured by shear force. Shear cracks can be seen in Fig. 12.

3.2 Interface slip values at failure

A slip should not be observed between steel beam and concrete slab in a full-composite action. However, there will be some amount of slip occurring at interface in ultimate loading conditions (see Fig. 13).

Strain distribution over cross-section must be linear. Strain values at top and bottom of cross-section could be unified by a single line and must be zero at neutral axis. Maximum strain values recorded in present study did not fulfill those requirements, therefore, there must be two neutral axes occurring in both slab and beam at failure. Strain at interface was determined by using recorded slips at interface in ultimate loading of composite beams. Slip samples can be seen in Fig. 14. Corresponding interface strains are given in Table 9 and strain distributions calculated at failure are presented in Fig. 15. Locations of neutral axis were given for E&K series beams in Table 10. These slip values are in compliance with the findings of Shariati *et al*. 2012, Xue *et al*. 2012, Maleki 2009.

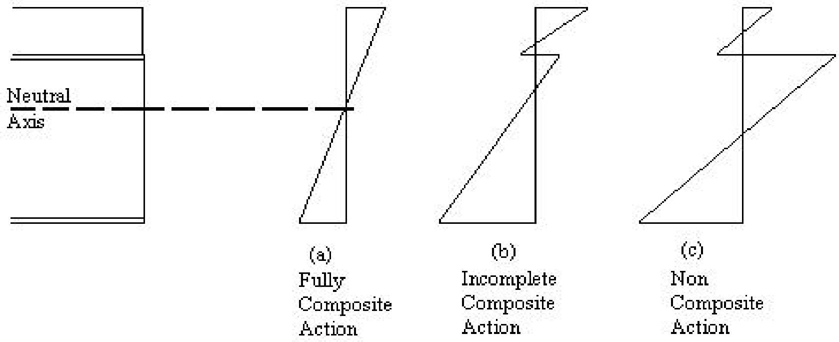

Fig. 13 Interaction between slab and beam (Davies 1975, Arda and Yardimci 2000, Knowles 1973, Salmon and Johnson 1971, Viest *et al*. 1958)

Table 9 Slip and Interface strain values

Specimen	Slip (mm)	Interface Strains
*E*1	5.5	0.0036
*E*2	7.5	0.0050
*E*3	7.0	0.0046
*E*4	6.0	0.0040
*K*1 (angle)	4.5	0.0030
*K*2 (box)	3.0	0.0020
*K*3 (stud)	6.5	0.0043
*K*4 (channel)	5.0	0.0033

Fig. 14 Slip of steel beams at ultimate load

The beam with channel connectors was exposed to step-by-step much more load with increasing loads. K3 had the highest deflection due to the highest strain. Effects of relatively long height of studs can clearly be seen while comparing K3 and K4 beams. Strain values were nearly the same at top of concrete, but because of stud's height and geometrical properties, strain distribution was well-arranged compared to K4. Larger cross-sectional areas of channels pull the neutral axis down. A similar case exists in *K*1 beams.

Table 10 Neutral axis locations of beams from top

Series	Beams	Neutral axis locations from top	
		Before Test	Failure
Encased sections	*E*1	77,1	70
	*E*2	81,6	60
	*E*3	86,1	55
	*E*4	81,8	70
Non-encased sections	*K*1	86,1	83
	*K*2	81,8	81
	*K*3	90,6	78
	*K*4	92,9	88

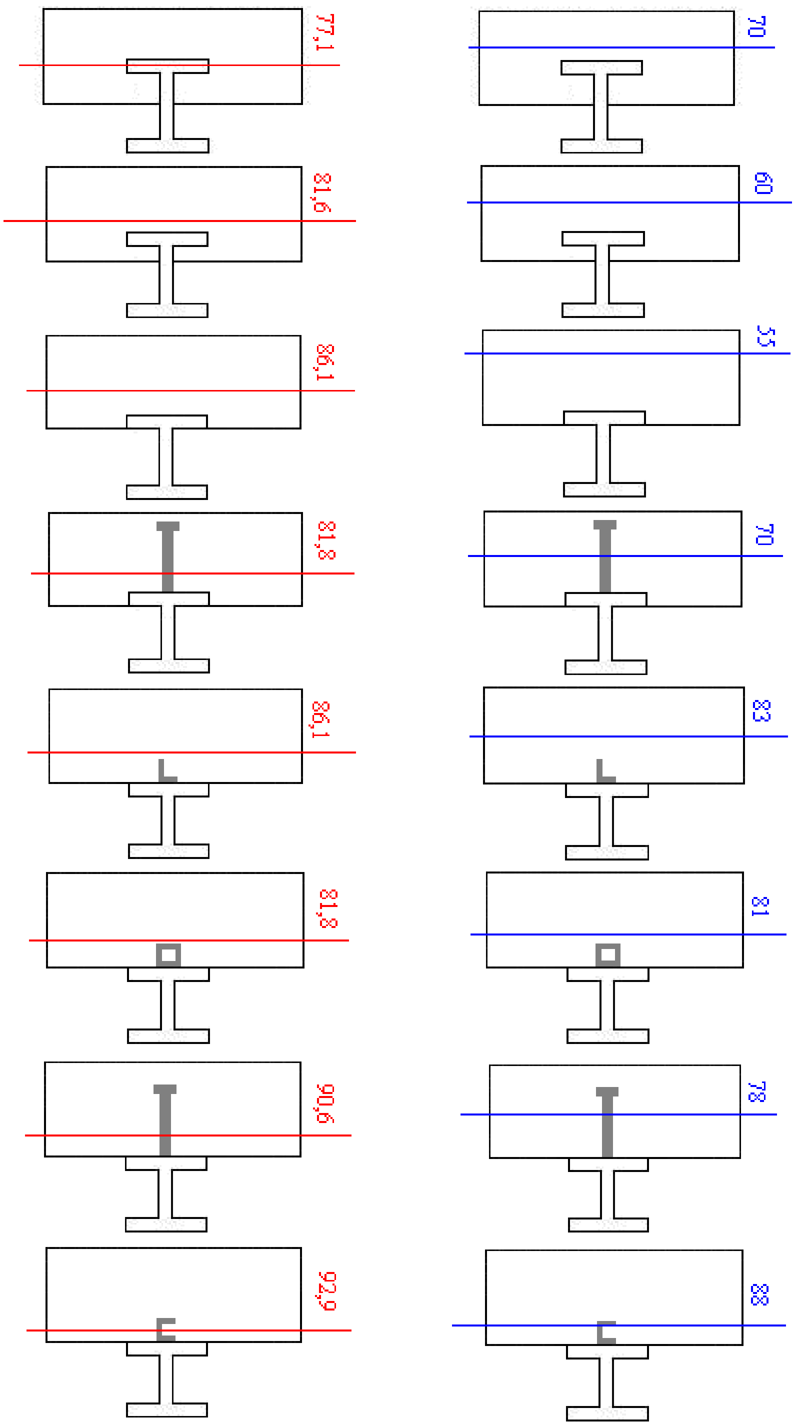

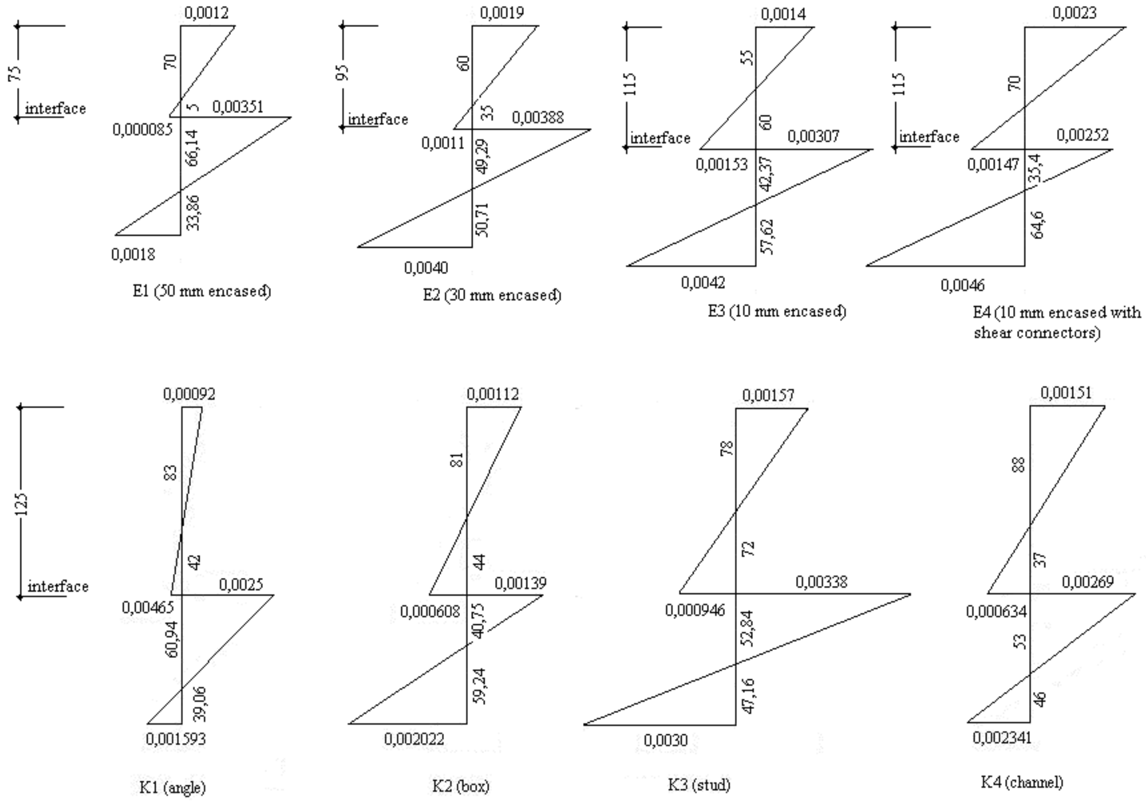

Fig. 15 Strain distribution of composite beams at failure

4. Conclusions

Bending behavior of reinforced concrete slabs encased over shallow I-sections at different levels of compression heads were investigated in present study.

Load bearing capacity of composite beams decreased with increasing embedment depths into concrete. Furthermore, deflection capacity also decreased with increasing embedment. When there is concern about load bearing capacity and deflection, increasing embedment was found to be more economic than using higher cross section I-profile steel beams.

The load bearing capacity increases and deflection stays nearly the same in composite beams with shear connectors compared to beams without shear connector.

In order to achieve the deflection limit in composite beams, either increasing beam cross section height or increasing embedding depth of concrete slab into the compression head of I-sections is necessary. The designer should reach the solution by taking both load bearing capacity and deflection capacity of composite beams into consideration.

Using short and broad-area shear connectors results in steel accumulation at bottom of the slab. Such accumulations yield rigid slabs. Like the ones in present study, steel beams were overloaded in shallow steel beam-thick slab case. Because of overloading, steel beam acts independently from the slab and yields earlier in increasing load levels. Increasing stresses causes slippages at interface and beam becomes unstable.

References

Amadio, C. and Fragiacomo, M. (2002), "Effective width evaluation of steel-concrete composite beams", *J. Construct. Steel Res.*, **58**(3), 373-388.

Ansourian, P. (1981), "Experiments on composite beams", *Proceeding of Institute of Civil Engineers - Part2*, **71**, 25-51.

Arda, T.S. and Yardimci, N. (2000), *Plastic design of composite member in steel structures*, Birsen Publishing, Istanbul, Turkey.

Byfield, M.P., Dhanalakshmi, M. and Goyder, H.G.D. (2004), "Modeling of undraped semi-continuous composite beams", *J. Construct. Steel Res.*, **60**(9), 1353-1367.

Cai, C.S., Nie, J. and Shi, X.M. (2007), "Interface slip effect on bonded plate repairs of concrete beams", *Eng. Struct.*, **29**(6), 1084-1095.

Chen, W.Q., Wu, Y.F. and Xu, R.Q. (2007), "State space formulation for composite beam-columns with partial interaction", *Compos. Sci. Tech.*, **67**(11-12), 2500-2512.

Chung, K.F. and Lawson, R.M. (2001), "Simplified design of composite beams with large web openings to Eurocode 4", *J. Construct. Steel Res.*, **57**(2), 135-163.

Dall'Asta, A. (2001), "Composite beams with weak shear connection", *Int. J. Solid. Struct.*, **38**(32-33), 5605-5624.

Davies, C. (1975), *Steel-Concrete Composite Beams for Buildings*, John Wiley & Sons.

Fabbrocino, G., Manfredi, G. and Cosenza, E. (2000), "Analysis of continuous composite beams including partial interaction and bond", *J. Struct. Eng. ASCE*, **126**(12), 1288-1294.

Fabbrocino, G., Manfredi, G. and Cosenza, E. (2001), "Ductility of composite beams under negative bending: An equivalence index for reinforcing steel classification", *J. Construct. Steel Res.*, **57**(2), 185-202.

Fabbrocino, G., Manfredi, G. and Cosenza, E. (2002), "Modelling of continuous steel-concrete composite beams: Computational aspects", *Comp. Struct.*, **80**(27-30), 2241-2251.

Fahmy, E.H. (1996), "Analysis of composite beams with rectangular web openings", *J. Construct. Steel Res.*, **37**(1), 47-62.

Galambos, T.V. (2000), "Recent research and design developments in steel and composite steel-concrete structures in USA", *J. Construct. Steel Res.*, **55**(1-3), 289-303.

Gattesco, N. (1999), "Analytical modeling of nonlinear behavior of composite beams with deformable connection", *J. Construct. Steel Res.*, **52**(2), 195-218.

Hamada, S. and Longworth, L. (1976), "Ultimate strength of continuous composite beams", *J. Struct. Div.*, **102**(7), 1463-1478.

Heins, C.P. and Fan, H.M. (1976), "Effective composite beam width at ultimate load", *J. Struct. Div.*, **102**(11), 2163-2179.

Johansen, R.P. (1970), "Research on steel-concrete composite beams", *J. Struct. Div. ASCE*, **96** (3), 445-459.

Johansen, R.P. and Willmington, R.T. (1972), "Vertical shear in continuous composite beams", *Proceeding of Institute of Civil Engineers*, 189-206.

Knowles, P.R. (1973), *Composite Steel and Concrete Construction*, John Wiley & Sons.

Lee, J. and Kim, S.E. (2010), "Flexural-torsional buckling of thin walled I-section composites", *Comput. Struct.*, **79**(10), 987-995.

Liang, Q.Q., Uy, B., Bradford, M.A. and Ronagh, H.R. (2004), "Ultimate shear strength of continuous composite beams in combined bending and shear", *J. Construct. Steel Res.*, **60** (8), 1109-1128.

Maleki, S. and Mahoutian, M. (2009), "Experimental and analytical study on channel shear connectors in fiber-reinforced concrete", *J. Construct. Steel Res.*, **65**(8-9), 1787-1793.

Mergulhao, A.J.R., Freitas, A.M.S. and Machado, R.M. (1998), "Composite steel beams strength evaluation constituted of steel profiles filled with reinforced concrete", *J. Construct. Steel Res.*, **46**(1-3), 223-224.

Nakamura, S.I. and Narita, N. (2003), "Bending and shear strengths of partially encased composite I girders", *J. Construct. Steel Res.*, **59**(12), 1435-1453.

Nie, J.G. and Cai, C.S. (2003), "Steel-concrete composite beams considering shear slip effects", *J. Struct. Eng. ASCE*, **129**(4), 495-506.

Ranzi, G., Gara, F. and Ansourian, P. (2006), "General method of analysis for composite beams with longitudinal and transverse partial interaction", *Comput. Struct.*, **84**(31-32), 2373-2384.

Ranzi, G. and Zona, A. (2007), "A steel-concrete composite beam model with partial interaction including the shear deformability of the steel component", *Eng. Struct.*, **29**(11), 3026-3041.

Salmon, C.G. and Johnson, J.E. (1971), *Steel Structures Design and Behavior*, Intext Educational Publishers.

Shanmugam, N.E., Ng, Y.H. and Liew, J.Y.R. (2002), "Behaviour of composite haunched beams connection", *Eng. Struct.*, **24**(11), 1451-1463.

Shariati, M., Sulong, N.H.R., Suhatril, M., Shariati, A., Arabnejad Khanouki, M.M. and Sinaei, H. (2012), "Behaviour of *C* shaped angle shear connectors under monotonic and fully reversed cycled loading: An experimental study", *Mater. Design*, **41**, 67-73.

Thevendran, V., Shanmugam, N.E., Chen, S. and Liew, J.Y.R. (2000), "Experimental study on steel-concrete composite beams curved in plan", *Eng. Struct.*, **22**(8), 877-889.

TS 3526 (1985), *Water Absorption and Unit Weight of Concrete Aggregates*, Institute of Turkish Standards, Ankara, Turkey.

TS 500 (2000), *Requirements for Design and Construction of Reinforced Concrete Structures*, Institute of Turkish Standards, Ankara, Turkey.

TS 706 (1985), *Standard of Gradation Sieves*, Institute of Turkish Standards, Ankara, Turkey.

TS 802 (1985), *Concrete Mixture Calculations*, Institute of Turkish Standards, Ankara, Turkey.

Viest, I.M., Fountain, R.S. and Singleton, R.C. (1958), *Composite construction in steel and concrete for bridges and buildings*, McGraw-Hill Book Company, New York, NY, USA.

Xue, D., Liu, Y., Yu, Z. and He, J. (2012), "Static behavior of multi-stud shear connectors for steel-concrete composite bridge", *J. Construct. Steel Res.*, **74**, 1-7.

DL